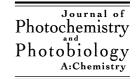


Journal of Photochemistry and Photobiology A: Chemistry 157 (2003) 323-326



www.elsevier.com/locate/jphotochem

Subject Index of Volume 157

Absorption

A critical review of the absorption cross-sections of O₃ and NO₂ in the ultraviolet and visible, 185

Absorption spectra

Measurements of molecular absorption spectra with the SCIAMACHY pre-flight model: instrument characterization and reference data for atmospheric remote-sensing in the 230–2380 nm region, 167

Acetaldehyde

The reaction of acetaldehyde and propional dehyde with hydroxyl radicals: experimental determination of the primary ${\rm H_2O}$ yield at room temperature, 269

A visible and FTIR spectrometric study of the nighttime chemistry of acetaldehyde and PAN under simulated atmospheric conditions, 283

Acetic acid (AA)

The solvent effect on the excited-state proton transfer of lumichrome, 5 Gas phase UV absorption spectra for peracetic acid, and for acetic acid monomers and dimers, 161

Acid Red 14

Photocatalytic degradation of azo dye acid red 14 in water: investigation of the effect of operational parameters, 111

Acridinedione dyes

Excited state behaviour of acridinedione dyes in PMMA matrix: inhomogeneous broadening and enhancement of triplet, 23

Advanced oxidation processes

Photocatalytic degradation of azo dye acid red 14 in water: investigation of the effect of operational parameters, 111

Ag deposition

Photoelectrochemical performance of Ag–TiO $_2$ /ITO film and photoelectrocatalytic activity towards the oxidation of organic pollutants, 71

Aqueous phase

Temperature-dependent kinetics studies of aqueous phase reactions of ${\rm SO_4}^-$ radicals with dimethylsulfoxide, dimethylsulfone, and methanesulfonate, 311

Arrhenius expression

A laser-induced fluorescence study of the $O(^3P)$ + CF_3I and IO + NO reactions. Evidence for an association channel for O + CF_3I at low temperatures, 223

Atmospheric chemistry

Kinetics of the reactions of the hydroxyl radical with CH_3OH and C_2H_5OH between 235 and 360 K, 237

Azo dyes

Photocatalytic degradation of azo dye acid red 14 in water: investigation of the effect of operational parameters, 111

Cadmium-zinc sulphide embedded in Whatman filter paper

Immobilisation of CdS, ZnS and mixed ZnS–CdS on filter paper. Effect of hydrogen production from alkaline Na₂S/Na₂S₂O₃ solution, 87

Carbazole

Cationic photopolymerization of carbazolyl-containing vinyl ethers, 117

Cation radical

Laser photolysis of pyrenesulfonate and pyrenetetrasulfonate via twophoton ionization in aqueous and reverse micellar solutions, 33

CFC

Measurements of the infrared absorption cross-sections of haloalkanes and their use in a simplified calculational approach for estimating direct global warming potentials, 211

4-Chlorophenol

Comparative photocatalytic degradation using natural and artificial UVlight of 4-chlorophenol as a representative compound in refinery wastewater, 103

Composite electrode

Influence of the mixed ratio on the photocurrent of the TiO₂/SnO₂ composite photoelectrodes sensitized by mercurochrome, 39

Continuous-scar

Time-windowing Fourier transform absorption spectroscopy for flash photolysis investigations, 127

Cross-section

New measurements of OCIO absorption cross-sections in the 325–435 nm region and their temperature dependence between 213 and 293 K 149

A critical review of the absorption cross-sections of O₃ and NO₂ in the ultraviolet and visible, 185

Degradation

On the atmospheric degradation of pyruvic acid in the gas phase, 295

Degradation of azo dye

Photoelectrocatalytic degradation of Remazol Brilliant Orange 3R on titanium dioxide thin-film electrodes, 55

Desulfonation

Laser photolysis of pyrenesulfonate and pyrenetetrasulfonate via two-photon ionization in aqueous and reverse micellar solutions,

2,4-Dinitrophenylhydrazine

Laboratory investigation of the photooxidation of formaldehyde combining FTIR analysis of stable species and HO₂ detection by the chemical amplifier technique, 275

Discharge-flow

Measurements of the temperature-dependent rate coefficient for the reaction $O(^3P) + NO_2 \rightarrow NO + O_2$, 231

Disinfection

Photocatalytic bactericidal effect of TiO₂ on *Enterobacter cloacae*. Comparative study with other Gram (–) bacteria, 81

DMS

Temperature-dependent kinetics studies of aqueous phase reactions of ${\rm SO_4}^-$ radicals with dimethylsulfoxide, dimethylsulfone, and methanesulfonate, 311

DMSC

The solvent effect on the excited-state proton transfer of lumichrome, 5 Temperature-dependent kinetics studies of aqueous phase reactions of SO₄ radicals with dimethylsulfoxide, dimethylsulfone, and methanesulfonate, 311

DMSO2

Temperature-dependent kinetics studies of aqueous phase reactions of ${\rm SO_4}^-$ radicals with dimethylsulfoxide, dimethylsulfone, and methanesulfonate, 311

Elsevier Science B.V. PII: S1010-6030(03)00140-0 324 Subject Index

EDTA

Laboratory investigation of the photooxidation of formaldehyde combining FTIR analysis of stable species and HO₂ detection by the chemical amplifier technique, 275

Electrolyte effects

Photoelectrocatalytic degradation of Remazol Brilliant Orange 3R on titanium dioxide thin-film electrodes, 55

Electron hole separation

Immobilisation of CdS, ZnS and mixed ZnS-CdS on filter paper. Effect of hydrogen production from alkaline Na₂S/Na₂S₂O₃ solution, 87 Elemental mercury

Gas phase elemental mercury: a comparison of LIF detection techniques and study of the kinetics of reaction with the hydroxyl radical, 247

Energy barrier

Influence of the mixed ratio on the photocurrent of the TiO₂/SnO₂ composite photoelectrodes sensitized by mercurochrome, 39

Enterobacter cloacae

Photocatalytic bactericidal effect of TiO₂ on *Enterobacter cloacae*. Comparative study with other Gram (–) bacteria, 81

Ethanol

Kinetics of the reactions of the hydroxyl radical with CH_3OH and C_2H_5OH between 235 and 360 K, 237

Excited-state proton transfer

The solvent effect on the excited-state proton transfer of lumichrome, 5

Fluorescence

Photodegradation of Nabumetone in aqueous solutions, 93

Formic acid

Photoelectrochemical performance of Ag-TiO₂/ITO film and photoelectrocatalytic activity towards the oxidation of organic pollutants, 71

Fourier transform spectroscopy

Time-windowing Fourier transform absorption spectroscopy for flash photolysis investigations, 127

Frontier orbitals

Frontier orbitals control in the reactivity of singlet oxygen with lignin model compounds. An ab initio study, 1

FTIR

A visible and FTIR spectrometric study of the nighttime chemistry of acetaldehyde and PAN under simulated atmospheric conditions, 283

FTIR analysis

Laboratory investigation of the photooxidation of formaldehyde combining FTIR analysis of stable species and HO₂ detection by the chemical amplifier technique, 275

FTIR spectroscopy

Photocatalytic decomposition of textile dyes on TiO₂-Tytanpol A11 and TiO₂-Degussa P25, 65

Photodegradation of Nabumetone in aqueous solutions, 93

Gas chromatography-mass spectrometry

Photodegradation of Nabumetone in aqueous solutions, 93

Gas phase UV absorption

Gas phase UV absorption spectra for peracetic acid, and for acetic acid monomers and dimers, 161

Gas-phase

Rate constants for the photolysis of the nitronaphthalenes and methylnitronaphthalenes, 301

Global warming potential

Measurements of the infrared absorption cross-sections of haloalkanes and their use in a simplified calculational approach for estimating direct global warming potentials, 211

Gram (-) bacilli

Photocatalytic bactericidal effect of TiO₂ on *Enterobacter cloacae*. Comparative study with other Gram (–) bacteria, 81

Halon

Measurements of the infrared absorption cross-sections of haloalkanes and their use in a simplified calculational approach for estimating direct global warming potentials, 211

H-atom abstraction

The reaction of acetaldehyde and propional dehyde with hydroxyl radicals: experimental determination of the primary $\rm H_2O$ yield at room temperature, 269

Heterogeneous photocatalysis

Photocatalytic bactericidal effect of TiO₂ on *Enterobacter cloacae*. Comparative study with other Gram (–) bacteria, 81

Heterogeneous reactions

Temperature-dependent kinetics studies of aqueous phase reactions of SO_4^- radicals with dimethylsulfoxide, dimethylsulfone, and methanesulfonate. 311

Higher photostability

Excited state behaviour of acridinedione dyes in PMMA matrix: inhomogeneous broadening and enhancement of triplet, 23

Hydrogen production

Immobilisation of CdS, ZnS and mixed ZnS-CdS on filter paper. Effect of hydrogen production from alkaline Na₂S/Na₂S₂O₃ solution, 87 Hydroxyl radical

Kinetics of the reactions of the hydroxyl radical with CH₃OH and C₂H₅OH between 235 and 360 K, 237

Kinetics and products of the reactions of OH radicals with 2-methyl-2-pentanol and 4-methyl-2-pentanol, 257

The reaction of acetaldehyde and propional dehyde with hydroxyl radicals: experimental determination of the primary $\rm H_2O$ yield at room temperature, 269

Hydroxylation

Laser photolysis of pyrenesulfonate and pyrenetetrasulfonate via twophoton ionization in aqueous and reverse micellar solutions, 33

1-(3-Hydroxy-2-pyridyl)-2-(pentamethyldisilanyl)ethyne

Photoreactions of 1-(3-hydroxy-2-pyridyl)-2-(pentamethyldisilanyl) ethyne, aza analogue of 1-o-hydroxyphenyl-2-(pentamethyldisilanyl)ethyne, 15

Infrared absorption cross-sections

Measurements of the infrared absorption cross-sections of haloalkanes and their use in a simplified calculational approach for estimating direct global warming potentials, 211

Infrared forcing

Measurements of the infrared absorption cross-sections of haloalkanes and their use in a simplified calculational approach for estimating direct global warming potentials, 211

Inhomogeneous broadening

Excited state behaviour of acridinedione dyes in PMMA matrix: inhomogeneous broadening and enhancement of triplet, 23

Iodine monoxide

A laser-induced fluorescence study of the $O(^3P)$ + CF_3I and IO + NO reactions. Evidence for an association channel for O + CF_3I at low temperatures, 223

Iodonium salt

Cationic photopolymerization of carbazolyl-containing vinyl ethers, 117 Iron–arene complex

Cationic photopolymerization of carbazolyl-containing vinyl ethers, 117

Kinetics

Kinetics of the reactions of the hydroxyl radical with CH₃OH and C₂H₅OH between 235 and 360 K, 237

Rate constants for the photolysis of the nitronaphthalenes and methylnitronaphthalenes, 301

Laser flash photolysis

Temperature-dependent kinetics studies of aqueous phase reactions of ${\rm SO_4}^-$ radicals with dimethylsulfoxide, dimethylsulfone, and methanesulfonate, 311

Subject Index 325

Laser photolysis

Laser photolysis of pyrenesulfonate and pyrenetetrasulfonate via twophoton ionization in aqueous and reverse micellar solutions, 33

Laser-induced fluorescence

A laser-induced fluorescence study of the O(³P) + CF₃I and IO + NO reactions. Evidence for an association channel for O + CF₃I at low temperatures, 223

Gas phase elemental mercury: a comparison of LIF detection techniques and study of the kinetics of reaction with the hydroxyl radical, 247

Lignin

Frontier orbitals control in the reactivity of singlet oxygen with lignin model compounds. An ab initio study, 1

Lumichrome

The solvent effect on the excited-state proton transfer of lumichrome, 5

Methanol

Kinetics of the reactions of the hydroxyl radical with CH_3OH and C_2H_5OH between 235 and 360 K, 237

Methylnitronaphthalenes

Rate constants for the photolysis of the nitronaphthalenes and methylnitronaphthalenes, 301

2-Methyl-2-pentanol

Kinetics and products of the reactions of OH radicals with 2-methyl-2pentanol and 4-methyl-2-pentanol, 257

4-Methyl-2-pentanol

Kinetics and products of the reactions of OH radicals with 2-methyl-2-pentanol and 4-methyl-2-pentanol, 257

MS

Temperature-dependent kinetics studies of aqueous phase reactions of SO_4^- radicals with dimethylsulfoxide, dimethylsulfone, and methanesulfonate, 311

Nabumetone

Photodegradation of Nabumetone in aqueous solutions, 93

Nanosized particle

Synthesis of photocatalytic ${\rm TiO_2}$ nanoparticles: optimization of the preparation conditions, 47

Nitrogen dioxide

Measurements of the temperature-dependent rate coefficient for the reaction $O(^3P)$ + $NO_2 \rightarrow NO$ + O_2 , 231

Nitronaphthalenes

Rate constants for the photolysis of the nitronaphthalenes and methylnitronaphthalenes, 301

Nitro-PAH

Rate constants for the photolysis of the nitronaphthalenes and methylnitronaphthalenes, 301

NO_2

A critical review of the absorption cross-sections of O₃ and NO₂ in the ultraviolet and visible, 185

O_3

A critical review of the absorption cross-sections of O₃ and NO₂ in the ultraviolet and visible, 185

OCIC

New measurements of OCIO absorption cross-sections in the 325–435 nm region and their temperature dependence between 213 and 293 K. 149

Organic dye degradation

Photocatalytic decomposition of textile dyes on TiO₂-Tytanpol A11 and TiO₂-Degussa P25, 65

Ozone

A critical review of the absorption cross-sections of O₃ and NO₂ in the ultraviolet and visible, 185

Peracetic acid

Gas phase UV absorption spectra for peracetic acid, and for acetic acid monomers and dimers, 161

Peroxyacetyl nitrate

A visible and FTIR spectrometric study of the nighttime chemistry of acetaldehyde and PAN under simulated atmospheric conditions, 283

Photocatalysis

Synthesis of photocatalytic ${\rm TiO_2}$ nanoparticles: optimization of the preparation conditions, 47

Photoelectrochemical performance of Ag-TiO₂/ITO film and photoelectrocatalytic activity towards the oxidation of organic pollutants, 71

Photocatalytic degradation of azo dye acid red 14 in water: investigation of the effect of operational parameters, 111

Photocatalyst

Comparative photocatalytic degradation using natural and artificial UVlight of 4-chlorophenol as a representative compound in refinery wastewater, 103

Photocurrent

Influence of the mixed ratio on the photocurrent of the TiO_2/SnO_2 composite photoelectrodes sensitized by mercurochrome, 39

Photodegradation

Photodegradation of Nabumetone in aqueous solutions, 93

Photocatalytic degradation of azo dye acid red 14 in water: investigation of the effect of operational parameters, 111

Photoelectrocatalysis

Photoelectrocatalytic degradation of Remazol Brilliant Orange 3R on titanium dioxide thin-film electrodes, 55

Photoelectrochemistry

Photoelectrochemical performance of Ag-TiO₂/ITO film and photoelectrocatalytic activity towards the oxidation of organic pollutants, 71

Photolysis

A laser-induced fluorescence study of the O(³P) + CF₃I and IO + NO reactions. Evidence for an association channel for O + CF₃I at low temperatures, 223

On the atmospheric degradation of pyruvic acid in the gas phase, 295 Rate constants for the photolysis of the nitronaphthalenes and methylnitronaphthalenes, 301

Photopolymerization

Cationic photopolymerization of carbazolyl-containing vinyl ethers, 117

PMMA matrix

Excited state behaviour of acridinedione dyes in PMMA matrix: inhomogeneous broadening and enhancement of triplet, 23

Pressure broadening

Measurements of the infrared absorption cross-sections of haloalkanes and their use in a simplified calculational approach for estimating direct global warming potentials, 211

Product distribution

The reaction of acetaldehyde and propional dehyde with hydroxyl radicals: experimental determination of the primary $\rm H_2O$ yield at room temperature, 269

Propionaldehyde

The reaction of acetaldehyde and propionaldehyde with hydroxyl radicals: experimental determination of the primary H₂O yield at room temperature, 269

Pulsed laser photolysis

Gas phase elemental mercury: a comparison of LIF detection techniques and study of the kinetics of reaction with the hydroxyl radical, 247 Pyrenesulfonates

Laser photolysis of pyrenesulfonate and pyrenetetrasulfonate via twophoton ionization in aqueous and reverse micellar solutions, 33

Pyruvic acid

On the atmospheric degradation of pyruvic acid in the gas phase, 295

Rate coefficients

A laser-induced fluorescence study of the O(³P) + CF₃I and IO + NO reactions. Evidence for an association channel for O + CF₃I at low temperatures, 223

326 Subject Index

Reaction kinetics

Kinetics and products of the reactions of OH radicals with 2-methyl-2pentanol and 4-methyl-2-pentanol, 257

Temperature-dependent kinetics studies of aqueous phase reactions of ${\rm SO_4}^-$ radicals with dimethylsulfoxide, dimethylsulfone, and methanesulfonate. 311

Reaction products

Kinetics and products of the reactions of OH radicals with 2-methyl-2pentanol and 4-methyl-2-pentanol, 257

Remote-sensing

New measurements of OCIO absorption cross-sections in the 325–435 nm region and their temperature dependence between 213 and 293 K, 149

Measurements of molecular absorption spectra with the SCIAMACHY pre-flight model: instrument characterization and reference data for atmospheric remote-sensing in the 230–2380 nm region, 167

Resonance fluorescence

Measurements of the temperature-dependent rate coefficient for the reaction $O(^3P) + NO_2 \rightarrow NO + O_2$, 231

Reverse micelle

Laser photolysis of pyrenesulfonate and pyrenetetrasulfonate via two-photon ionization in aqueous and reverse micellar solutions, 33

Review

A critical review of the absorption cross-sections of O₃ and NO₂ in the ultraviolet and visible, 185

SCIAMACHY

Measurements of molecular absorption spectra with the SCIAMACHY pre-flight model: instrument characterization and reference data for atmospheric remote-sensing in the 230–2380 nm region, 167

1-Silaallene

Photoreactions of 1-(3-hydroxy-2-pyridyl)-2-(pentamethyldisilanyl) ethyne, aza analogue of 1-o-hydroxyphenyl-2-(pentamethyldisilanyl)ethyne, 15

Silacyclopropene

Photoreactions of 1-(3-hydroxy-2-pyridyl)-2-(pentamethyldisilanyl) ethyne, aza analogue of 1-o-hydroxyphenyl-2-(pentamethyldisilanyl)ethyne, 15

Singlet oxygen

Frontier orbitals control in the reactivity of singlet oxygen with lignin model compounds. An ab initio study, 1

SO_4

Temperature-dependent kinetics studies of aqueous phase reactions of ${\rm SO_4}^-$ radicals with dimethylsulfoxide, dimethylsulfone, and methanesulfonate, 311

Sol-gel route

Synthesis of photocatalytic ${\rm TiO_2}$ nanoparticles: optimization of the preparation conditions, 47

Spectro-electrochemistry

Influence of the mixed ratio on the photocurrent of the TiO₂/SnO₂ composite photoelectrodes sensitized by mercurochrome, 39

Spectroscopy

New measurements of OCIO absorption cross-sections in the 325–435 nm region and their temperature dependence between 213 and 293 K, 149

Stratospheric ozone

Measurements of the temperature-dependent rate coefficient for the reaction $O(^3P) + NO_2 \rightarrow NO + O_2$, 231

Structure activity relationships

Atmospheric fate of small alkoxy radicals: recent experimental and theoretical advances, 137

Sulfonium salt

Cationic photopolymerization of carbazolyl-containing vinyl ethers, 117 Sunlight

Comparative photocatalytic degradation using natural and artificial UVlight of 4-chlorophenol as a representative compound in refinery wastewater, 103

Temperature dependence

Temperature-dependent kinetics studies of aqueous phase reactions of ${\rm SO_4}^-$ radicals with dimethylsulfoxide, dimethylsulfone, and methanesulfonate, 311

Time-resolved spectroscopy

Time-windowing Fourier transform absorption spectroscopy for flash photolysis investigations, 127

TiO_2

Photoelectrochemical performance of Ag-TiO₂/ITO film and photoelectrocatalytic activity towards the oxidation of organic pollutants, 71

Photocatalytic bactericidal effect of TiO₂ on *Enterobacter cloacae*. Comparative study with other Gram (–) bacteria, 81

TiO2 thin-film electrode

Photoelectrocatalytic degradation of Remazol Brilliant Orange 3R on titanium dioxide thin-film electrodes, 55

Titanium dioxide

Synthesis of photocatalytic TiO₂ nanoparticles: optimization of the preparation conditions, 47

Photocatalytic decomposition of textile dyes on TiO₂-Tytanpol A11 and TiO₂-Degussa P25, 65

Comparative photocatalytic degradation using natural and artificial UVlight of 4-chlorophenol as a representative compound in refinery wastewater, 103

Photocatalytic degradation of azo dye acid red 14 in water: investigation of the effect of operational parameters, 111

Trace gases

Measurements of molecular absorption spectra with the SCIAMACHY pre-flight model: instrument characterization and reference data for atmospheric remote-sensing in the 230–2380 nm region, 167

Triplet enhancement

Excited state behaviour of acridinedione dyes in PMMA matrix: inhomogeneous broadening and enhancement of triplet, 23

Troposphere

The reaction of acetaldehyde and propional dehyde with hydroxyl radicals: experimental determination of the primary $\rm H_2O$ yield at room temperature, 269

Tropospheric oxidation

Atmospheric fate of small alkoxy radicals: recent experimental and theoretical advances, 137

Unimolecular decomposition rate constant

Atmospheric fate of small alkoxy radicals: recent experimental and theoretical advances, 137

UV-Vis absorption spectroscopy

Photodegradation of Nabumetone in aqueous solutions, 93

Vinyl ether

Cationic photopolymerization of carbazolyl-containing vinyl ethers, 117